arXiv:astro-ph/0102195v1 12 Feb 2001

Evolution of Power Spectrum in Non-Gaussian Models

Naoki Seto

Department of Earth and Space Science, Osaka University, Toyonaka 560-0043

ABSTRACT

Evolution of power spectrum is studied for non-Gaussian models of structure formation. We generalize the dark-matter-approach to these models and find that the evolved spectrum at weakly nonlinear regime is mainly determined by a simple integral of the dark-matter-halo mass function in this approach. We also study the change of the nonlinear spectrum within the current observational constraint of the primordial non-Gaussianity.

Subject headings: cosmology: theory — large-scale structure of universe

1. INTRODUCTION

The power spectrum (or equivalently, the two-point correlation function as its Fourier transform) is the most fundamental measure to quantify matter clustering. Observational determination of it will bring us basic information of our universe. For example we can make constraints on cosmological parameters or on statistical aspects of the initial matter fluctuations that are the seeds of structure formation. Evolution of power spectrum by gravitational instability is also an interesting problem of nonlinear physics.

It is often assumed that the initial density fluctuations obey random Gaussian distributions. Though this is the simplest assumption from statistical point of views, its origin is explained by the simplest inflation scenario. Many analyses of the large-scale structure (LSS) in the universe are performed under this assumption. But other models (including some inflationary models and defect models) predict non-Gaussian initial fluctuations (Vilenkin 1985, Vachaspati 1986, Srednicki 1993, Peebles 1997, Linde & Mukahanov 1997) and possibilities of these models should be observationally investigated and have recently called much attentions (*e.g.* Peebles 1999a, 1999b, Ferreira, Górski & Magueijo 1998, Robinson, Gawiser & Silk 1998, 2000, Koyama, Soda & Taruya 1999, Willick 2000). These recent analyses involve the large-scale structure, properties (*e.g.* time evolution, spatial clustering) of clusters and CMB anisotropies. It now becomes clear that defect models cannot generate the observed CMB data by their own account but inflation models can explain them well (*e.g.* Albrecht

2000). Recent CMB data by BOOMERanG (Lange et al. 2000) and MAXIMA (Balbi et al. 2000) seem to suggest a weaker secondary peak than expected in a simple inflation scenario. Bouchet et al. (2000) discussed that this might be resolved by a hybrid scenario (inflation+cosmic string) in which some component of perturbations come from topological defects.

As for the quantitative measurement of the primordial non-Gaussianity, Contaldi et al. (2000) studied the third-order moment of the temperature anisotropies using 4yr COBE Differential Microwave Radiometer (DMR) data and found their most conservative estimate as $\langle(\Delta T)^3\rangle = -6.5 \pm 8.7[10^4\mu\mathrm{K}^3]$ (95% CL). Even though the magnitude of the error bar is large due to the limited sensitivity and angular resolution, traditional Gaussian model ($\langle(\Delta T)^3\rangle = 0$) is consistent with their result. Feldman et al. (2000) analyzed the bispectrum of the IRAS PSCz catalog (Saunders et al. 2000) and obtained a constraint for the primordial dimensionless skewness as $S \equiv \langle\delta^2\rangle / \langle\delta^2\rangle^{3/2} < 0.52$ (95% CL) for χ^2_N-models. Physics of CMB are much simpler than that of the galaxy distribution. The signal of the primordial non-Gaussianity could be masked by effects of biasing or nonlinear gravitational evolution (Verde et al. 2000). Observed data of both CMB and LSS will be significantly improved from MAP and Plank satellites, SDSS and 2dF surveys. Verde et al. (2000) insisted that CMB would be a better probe of the primordial non-Gaussianity for several non-Gaussian models and LSS data would be useful to constrain the biasing if primordial Gaussianity is suggested by CMB map.

So far nonlinear effects of matter clustering from non-Gaussian initial conditions are studies by numerical simulations (White 1999, Robinson & Baker 2000 and references therein) or by perturbative methods (*e.g.* Fry & Scherrer 1994, Chodorowski & Bouchet 1996, Scoccimarro 2000, Durrer et al. 2000). In this article we study evolution of the matter power spectrum for non-Gaussian models using the dark-matter-halo approach that can be traced back to Peebles (1974) and McClelland and Silk (1977) (see also Scherrer & Bertschinger 1991). For Gaussian models this approach is confirmed to reproduce numerical results very well from linear to nonlinear scales and regarded as an excellent tool to explore the matter clustering. It seems interesting to see how the nonlinear spectrum can be different within the currently allowed region of the primordial non-Gaussianity.

Many works have been recently performed with this approach for Gaussian models. For example nonlinear evolution of the power spectrum or the bispectrum of density field is studies by Ma & Fry (2000a, 2000b, 2000c), Seljak (2000), White (2000), Peacock & Smith (2000), Scoccimarro et al. (2000) and weak lensing effects by Cooray, Hu & Miralda-Escude (2000) and Cooray & Hu (2000). Komatsu & Kitayama (1999) investigated the Sunyaev & Zeldovich effect using a similar method. Here we simply extend this approach

to non-Gaussian models. This approach is made from three basic ingredients (i) the mass function of dark-matter-halos, (ii) the bias parameter of halos relative to the large-scale density fluctuations and (iii) the density profile of halos. Numerical analysis (Robinson & Baker 2000) supports that a straightforward extension of the Press & Schechter (1974) mass function is effective for non-Gaussian models. But validity of simple extensions of two other elements have not been checked numerically. Therefore we make a careful analysis and limit our investigation in the range where results are expected not to depend largely on the details of these two elements. Our goals in this article are set to the following two points. Firstly, we intend to roughly understand the effects of primordial non-Gaussianity on the weakly nonlinear evolution of the power spectrum. Secondary, we estimate the difference of the evolved spectra within the current observational constraint of the primordial non-Gaussianity.

This article is organized as follows. In §2 we describe basic properties of the dark-matter-halo approach with its basic three ingredients, namely, the mass function of halos (§2.1), the bias parameter (§2.2) and the density profiles of halos (§2.3). In §3 we analyze toy models to clarify the general effects of non-Gaussianity on the weakly nonlinear evolution of power spectrum. In §4 we investigate realistic models. We study a flat Λ-dominated model ($\Omega_0 = 0.3, \lambda_0 = 0.7$ and $h = 0.7$) with a fixed linear CDM spectrum and evaluate evolution of power spectra for log-normal probability distribution functions that are motivated by work of Robinson & Baker (2000). §5 is devoted to a brief summary. In appendix A we discuss the scale dependence of the skewness parameter for χ^2_N-models.

2. DARK MATTER HALO APPROACH

In the dark-matter-halo approach the nonlinear density field is given by superposition of halos with various masses. The density profile of each halo is assumed to be determined by its mass. The nonlinear power spectrum $P_{NL}(k)$ is constituted by two terms as

$$P_{NL}(k) = P_{2h}(k) + P_{1h}(k). \tag{1}$$

The two-halo term $P_{2h}(k)$ counts contributions of two points coming from two different halos and is given by

$$P_{2h}(k) \equiv \left[\rho_b^{-1} \int dm N(m) m b(m) u(k,m)\right]^2 P_L(k), \tag{2}$$

where $P_L(k)$ is the linear power spectrum. The one-halo term $P_{1h}(k)$ counts two particles within the same halo

$$P_{1h}(k) \equiv \rho_b^{-2} \int dm N(m) m^2 u(k,m)^2. \tag{3}$$

In the above equations ρ_b is the background density of the universe and $N(m)dm$ is the number density (mass function) of halos with mass from m to $m + dm$. The factor $b(m)$ is the bias parameter and represents distribution of halos relative to the large-scale density fluctuations. The function $u(k, m)$ is the Fourier transform of the density profile of a dark-matter-halo with mass m. The original form of the dark-matter halo approach was proposed by Peebles (1974). This approach has recently called much attention as our understandings of its ingredients have largely developed. In the following three subsections we study these basic ingredients.

2.1. Mass Function

We use the Press & Schechter (1974) formalism for the mass function $N(m)$ of collapsed objects. This formalism was first given for Gaussian random fields but can be straightforwardly extended to general models (*e.g.* Lucchin & Matarrese 1989, Chiu, Ostriker & Strauss 1998, Koyama, Soda & Taruya 1999, Robinson, Gawsier & Silk 2000, Willick 2000, Matarrese, Verde & Jimenez 2000). For simplicities we assume that the linear one-point probability distribution function (hereafter PDF) $p(\delta, \sigma)$ for the smoothed density field is written as

$$p(\delta, \sigma)d\delta = \sigma^{-1}p(\delta/\sigma)d\delta, \tag{4}$$

which means that the shape of the PDF is scale invariant. This ansatz is correct for the random Gaussian fluctuations, but not guaranteed for general non-Gaussian models. We comment on this scale dependence in §4 and appendix A.

The volume fraction of points that belong to collapsed objects with mass larger than m is given as follows

$$F^{-1}\int_{\delta_c/\sigma(m)}^{\infty} p(\nu)d\nu, \tag{5}$$

where $\delta_c \simeq 3(12\pi)^{2/3}/20 = 1.69$ is the critical linear density contrast for the spherical top-hat collapse and $\sigma(m)$ is the root-man-square mass fluctuation in a sphere of mass scale m. F is the normalization factor to account for all masses in the universe

$$F = \int_0^{\infty} p(\nu)d\nu. \tag{6}$$

For a symmetric profile $p(-\nu) = p(\nu)$ we have $F = 1/2$ (see also Bond et al. 1991, Lacey & Cole 1993). From equation (5) the number density of halos with mass from m to $m + dm$ is given as

$$N(m)dm = -F^{-1}\rho_b m^{-1}\frac{\partial}{\partial m}\int_{\delta_c/\sigma(m)}^{\infty} p(\nu)d\nu = -F^{-1}\rho_b p(\nu)m^{-1}\nu\frac{d\ln\sigma(m)}{dm}, \tag{7}$$

where we have denoted the normalized density contrast $\nu \equiv \delta_c/\sigma(m)$. We define the nonlinear mass m_* by equation $\sigma(m_*) = \delta_c$. For power-law models with $P_L(k) \propto k^n$ the linear mass fluctuation $\sigma(m)$ is given as

$$\sigma(m) = \delta_c \left(\frac{m}{m_*}\right)^{-(n+3)/6}. \tag{8}$$

In this subsection we have followed the basic analysis of the Press & Schechter method. For random Gaussian fluctuations some refinements have been proposed to reproduce N-body data better (*e.g.* Sheth & Tormen 1999, Jenkins et al. 2000). If we write down the mass function in the following form

$$N(m) = -A\sqrt{\frac{2}{\pi}}\alpha \frac{d\ln\sigma}{d\ln m}\frac{\rho_b}{m^2}\nu e^{-\alpha\nu^2/2}(1+(\alpha\nu^2)^{-p}). \tag{9}$$

The original Press & Schechter function corresponds to $(A, p, \alpha) = (0.5, 0, 1)$. The mass function given by Sheth & Tormen is given by parameters $(A, p, \alpha) = (0.322, 0.3, 0.707)$.

Robinson & Baker (2000) have recently confirmed that the simple extension of the Press & Schecheter formula (7) can accurately fit the mass function of clusters for several non-Gaussian models with typical error $\sim$ 25 percent (see also Avelino & Viana 2000). This result encourages our analytical study.

2.2. Bias Parameter

Next we study the bias parameter $b(m)$ using (i) the peak-background splitting method (Kaiser 1984) and (ii) a simple extension of the Press & Schechter method (Mo & White 1997, Mo, Jing & White 1997, Sheth & Lemson 1999, Sheth & Tormen 1999). When a large-scale perturbation δ_{LS} is added to the local (small scale) density field $\delta_{SS}(\boldsymbol{x})$, the density contrast for $\delta_{SS}(\boldsymbol{x})$ that is critical to the spherical top-hat collapse becomes $\delta_c - \delta_{LS}$. Then the Eulerian bias parameter for halos with mass m becomes (Mo & White 1997, Robinson, Gawiser & Silk 1998, Koyama, Soda & Taruya 1999)

$$b(m) = 1 - \frac{d\ln N(m)}{d\delta_c} = 1 - \frac{1}{\delta_c}\left(\frac{p'(\nu)}{p(\nu)}\nu + 1\right). \tag{10}$$

From equations (7) and (10) we can easily confirm the following equation [1]

$$\rho_b^{-1}\int_0^\infty b(m)N(m)m dm = 1. \tag{11}$$

[1]This equation holds for general non-scaling PDF in the form $p(\delta, \sigma)$.

As we see in §4 this equation is useful to know the behavior of the nonlinear power spectrum $P_{NL}(k)$ at large scale (small k). There are several analytical works about the bias parameter for non-Gaussian models (Robinson, Gawiser & Silk 1998, Koyama, Soda & Taruya 1999). But validity of the formulas (10) for a non-Gaussian PDF have not been checked with numerical simulations. But we expect that it works well, as this formula is simply derived from the Press & Schechter method that has been checked numerically for some non-Gaussian models as commented in the previous subsection.

For the mass function (9) given for random Gaussian fluctuations we have

$$b(\nu) = 1 + \frac{\alpha\nu^2 - 1}{\delta_c} + \frac{2p}{\delta_c(1 + (\alpha\nu^2)^p)}. \tag{12}$$

2.3. Density Profile of Dark Matter Halo

Recent numerical simulations suggest that the average density profile of cold-dark-mater (CDM) halos has nearly universal shape $\rho_m(r)$ characterized by its mass m (Navarro, Frenk & White 1996, 1997, Moore et al. 1998, 1999, Kravsov et al. 1998, Fukushige & Makino 1998, Jing & Suto 2000). These numerical simulations are performed with Gaussian initial conditions, but here we assume that the density profile depends only weakly on the linear PDF as the halo profile would strongly reflect nonlinear gravitational dynamics rather than the initial conditions. This assumption may be a potential weakness of our dark-matter-halo approach especially at strongly nonlinear regimes. However as we see in §4, the power spectrum $P_{NL}(k)$ at weakly nonlinear regimes does not depend details of the halo profile. In this article we adopt the universal profile of dark matter halo given in Navarro, Frenk & White (1997) as follows

$$u_m(r) \equiv \frac{\rho_m(r)}{m} \tag{13}$$

$$= \frac{fc^3}{4\pi R_{vir}^3} \frac{1}{(cr/R_{vir})^{-\alpha}(1 + cr/R_{vir})^{3+\alpha}}, \tag{14}$$

where R_{vir} is the virial radius of the halo. The halo mass m is written by R_{vir} as $m = 4\pi R_{vir}^3 \rho_b \Delta/3$ with the average density contrast $\Delta = 200$ (Einstein de-Sitter model) and $\Delta = 340$ (flat model with $\Omega_0 = 0.3$ and $\lambda_0 = 0.7$). The concentration parameter c determines the transition of inner and outer regions of a halo and depends on its mass m, roughly reflecting the formation epoch of the halo (Ma & Fry 2000b). We have $c = \beta(n)\sigma(m)$ with a coefficient $\beta(n)$ that depends on the linear power spectrum. The normalization factor f in equation (14) is given by

$$f = (\ln(1 + c) - c/(1 + c))^{-1}. \tag{15}$$

The density profile (14) in central region becomes $\rho(r) \propto r^{\alpha}$. The original result in Navarro, Frenk & White (1996) was $\alpha = -1$. But some other simulations show different results. For example, Moore et al. (1998, 1999) found $\alpha = -1.5$ and Jing & Suto (2000) argued that the index α is not a universal value but depends on the mass scale of halos. As we see later, the nonlinear evolution of power spectrum in weakly nonlinear regime is not sensitive to the details of the halo profile (see also Seljak 2000). Thus we use $\alpha = -1$ in this article.

Finally the Fourier transformed function $u(k, m)$ is defined in terms of the real space density profile $u_m(r)$ as

$$u(k,m) = \int d^3x \exp(-i\boldsymbol{x}\cdot\boldsymbol{k})u_m(r) \tag{16}$$

$$= 4\pi \int \frac{\sin kr}{kr} r^2 u_m(r) dr. \tag{17}$$

For the profile (14) an explicit analytic formula of $u(k, m)$ was given by Scoccimarro et al. (2000). At small wave number k the above Fourier transformation becomes a simple volume integral and we have $u(0, m) = 1$ due to the definition of $u_m(r)$ given in equation (13).

3. TOY MODELS

In this section we discuss effects of initial non-Gaussianity on the evolution of the power spectrum in Einstein de-Sitter background. We intend to extract out their general relations. From this standpoint we do not try to mimic realistic PDFs so seriously but study toy models that are different from Gaussian distribution. We also limit our analysis to scale-free initial spectra. With results obtained in this section we study models relevant for observational cosmology in §4.

3.1. Density Distribution Functions

We use the following four PDFs for the linear smoothed density fields. As commented in §2.1 we assume that the PDFs are scale invariant. The first example is the standard Gaussian model (G-model),

$$p_G(\nu) = \frac{1}{\sqrt{2\pi}} \exp\left(-\frac{\nu^2}{2}\right) \qquad -\infty < \nu < \infty. \tag{18}$$

This PDF is symmetric around the mean density $\nu = 0$ and we have $F = 0.5$. Here the factor F is defined in equation (6).

The second example is the Chi-square (χ^2)-model (C-model) with two degrees of freedom. A χ^2-model is often adopted as a typical non-Gaussian model and its origin in cosmological context was recently proposed by Peebles (1999a) using an inflation model. The PDF for the unsmoothed field is

$$p_C(\nu) = \begin{cases} \exp(-\nu - 1) & (-1 < \nu < \infty), \\ 0 & (\nu \leq -1), \end{cases} \tag{19}$$

with $F = 1/e$. We should notice that the PDF for the smoothed density field is same as the above unsmoothed one. This point is discussed in the next section and appendix A.

Next example is a log-normal distribution. This distribution is characterized by a parameter $\alpha(\geq 0)$ as follows

$$p_{LN}(\nu, \alpha) = \begin{cases} \dfrac{\alpha}{(1+\nu\alpha)\sqrt{2\pi \ln(1+\alpha^2)}} \exp\left[-\dfrac{\left\{\ln(\sqrt{1+\alpha^2}(1+\nu\alpha))\right\}^2}{2\ln(1+\alpha^2)} \right] & -\alpha^{-1} < \nu < \infty, \\ 0 & \nu \leq -\alpha^{-1}. \end{cases} \tag{20}$$

At $\alpha = 0$ we recover the Gaussian distribution $p_G(\nu) = p_{LN}(\nu, 0)$. The normalization factor F for this distribution is given in terms of the error function as

$$F = \frac{1}{2}\mathrm{erfc}\left[\frac{1}{2}\sqrt{\frac{\ln(1+\alpha^2)}{2}} \right], \tag{21}$$

where the error function is defined as $\mathrm{erfc}(x) = \sqrt{2/\pi}\int_x^\infty \exp(-y^2/2)dy$.

Here we add two models generated from equation (20). We define the LN1-model by

$$p_{LN1}(\nu) = p_{LN}(\nu, 1) \tag{22}$$

This profile has larger positive tail than the G-model. We have $F = 0.3386$. The final example (LN2-model) is obtained by a simple replacement of the previous model as

$$p_{LN2}(\nu) \equiv p_{LN1}(-\nu) = p_{LN}(-\nu, 1). \tag{23}$$

Note that we have $p_{LN2}(\nu) = 0$ for $\nu > 1$. Existence of halos with mass larger than m_* is prohibited in this model. As we see in the following section, the shape of the positive tail is very important to study nonlinear evolution of the power spectrum. The probability for $\nu \geq 3$ is 1.34×10^{-3} (G-model), 1.83×10^{-2} (C-model), 1.87×10^{-2} (LN1-model) and 0 (LN2-model). For $\nu \geq 5$ we have 2.87×10^{-7} (G-model), 2.48×10^{-3} (C-model), 5.11×10^{-3} (LN1-model) and 0 (LN2-model). We can easily confirm that all of these models have vanishing means

$$\langle \nu \rangle = \int_{-\infty}^{\infty} \nu p(\nu) d\nu = 0, \tag{24}$$

and are normalized properly

$$\int_{-\infty}^{\infty} p(\nu)d\nu = 1, \quad \left\langle \nu^2 \right\rangle = \int_{-\infty}^{\infty} \nu^2 p(\nu)d\nu = 1. \tag{25}$$

The skwness parameter $S \equiv \left\langle \nu^3 \right\rangle / \left\langle \nu^2 \right\rangle^{3/2}$ is a fundamental measure to characterize PDFs. [2] We have $S = 0$ (G-model), 2 (C-model), 4 (LN1-model) and -4 (LN2-model). For the general log-normal distribution $p_{LN}(\nu, \alpha)$ we have

$$S_{LN} = \alpha(3 + \alpha^2). \tag{26}$$

We use this relation in section 4.

3.2. Results

Using ingredients described in §2 and various linear PDFs given in §3 we calculate the nonlinear power spectrum $P_{NL}(k)$ with equations (1), (2) and (3). We use power-law models for initial spectra

$$P_L(k) = Ak^n, \tag{27}$$

where A is the normalization factor but irrelevant for present analysis. Time evolution of power spectrum can be reduced to rescaling of spatial length due to our scale-free initial conditions. We introduce the nonlinear wave-number k_{NL} that is defined by

$$\frac{1}{2\pi^2} \int_0^{k_{NL}} P_L(k)k^2 dk = 1. \tag{28}$$

This wave-number is the most fundamental scale for the present analysis. In this article we call the weakly nonlinear scale for the wave number k

$$0 < k \leq k_{NL}. \tag{29}$$

We first calculate the nonlinear power spectra $P_{NL}(k)$ for random Gaussian fields and compare our analytical predictions with fitting formula that is obtained from N-body simulations with the same Gaussian initial conditions (Peacock & Dodds 1996, see also Hamilton et al. 1991, Jain, Mo & White 1995). We fix the coefficient $\beta(n) = 3$ for the concentration parameter $c(m)$, but our results are insensitive to this parameter. It is found that our

[2]Definition of skewness parameter is different from that usually used for Gaussian initial condition (Bouchet et al. 1992).

model cannot reproduce the numerical results for spectral index with $n = 0$ in contrast to the case with $n \lesssim -1$. We can see this tendency from figures 1.a to 1.c. It is not clear why this dependence appears. Note that the evolved spectrum (thick solid line) for $n = -1$ obtained from the fitting formula is smaller than the linear spectrum (dash-dotted line) as predicted by the second-order perturbation theory (*e.g.* Makino, Sasaki & Suto 1992). In the framework of the dark-matter-halo approach this fact might be related to the possibility that the total halo mass fraction does not converge to unity (Jenkins et al. 2000) and the constraint (11) does not hold. As we see below, without the constraint (11) the two-halo term $P_{2h}(k)$ can be smaller than the linear spectrum $P_L(k)$ with nonnegligible amount at weakly nonlinear scale.

Here we limit our analysis for spectral indexes with $n \leq -1$ where our approach is expected to work well. These are close to the effective slope of a typical CDM power spectrum at weakly nonlinear regime $\sigma \lesssim 1$. In figures 1.a to 1.c we plot the nonlinear power spectrum $P_{NL}(k)$ in the form $\Delta(k)$ defined by

$$\Delta(k) \equiv \frac{P_{NL}(k)k^3}{2\pi^2}, \tag{30}$$

for spectral indexes $n = -2, -1.5$ and -1. In these figures contributions from the one-halo term $P_{1h}(k)$ and the two-halo term $P_{2h}(k)$ are presented separately. Note that our analytical prediction for the Gaussian models reproduce the results from N-body simulations well in the range $k \leq k_{NL}$ for $n \leq -1.5$ This fact indicates validity of the dark-matter-halo approach. For $n = -2$ model we also evaluate the nonlinear spectrum with using generalized formulas (9) (12) as in Seljak (2000). Our results shows good agreement with this results. in figures 1.a to 1.c w have used the fitting formula of Peacock & Dodds (1996). We find that the fitting formula of Jain et al. (1995) agrees with our analytical result better for $n = -2$ model but worse for $n = -1$ model.

Next we discuss behavior of the nonlinear power spectrum $P_{NL}(k)$ for various PDFs given in §3.1. We present numerical results in figures 1.a to 1.c. These are obtained by fully using the dark-matter-halo approach. In this calculation we evaluate all the three elements, the mass function $N(M)$, the bias parameter $b(M)$ and the halo profile $u(k, M)$. But information of the mass function is most important at weakly nonlinear regime, as we see below.

For all models the two-halo term in the range $k \lesssim k_{NL}$ is almost same as the linear power spectrum $P_L(k)$, as shown on figures for the two-halo term. In this regime we have $u(k, m) \simeq 1$ in the dominant contribution of the integral in equation (2) (see also figure 2).

Then we obtain the following relation from equation (11)

$$\int_0^\infty dmN(m)mb(m)u(k,m) \simeq \int_0^\infty dmN(m)mb(m) = \rho_b, \tag{31}$$

and

$$P_{2h}(k) \simeq P_L(k), \tag{32}$$

(see also Sheth et al. (2000) for a same kind of analysis for the two-point correlation function).

Therefore we can roughly understand the weakly nonlinear evolution of power spectrum only by analyzing the one-halo term

$$P_{1h}(k) = \rho_b^{-2} \int m^2 N(m) u(k,m)^2 dm. \tag{33}$$

As shown in figures 1.a to 1.c, the contribution of $\Delta(k)$ from one-halo term $P_{1h}(k)k^3/(2\pi^2)$ is nearly on a straight line proportional to k^3. This means $P_{1h}(k) \simeq const$ and indicates that k-dependence caused by the halo profile $u(k,m)$ is weak. Thus we approximate the one-halo term at weakly nonlinear regimes $k \lesssim k_{NL}$ by setting $u(k,m) = 1$

$$P_{1h}(k) \simeq P_{1h}(0) = \rho_b^{-2} \int dmN(m)m^2. \tag{34}$$

We have a constraint for the function $mN(m)$ due to the conservation of mass as

$$\int_0^\infty dmN(m)m = \rho_b, \tag{35}$$

and $P_{1h}(0)$ in equation(34) becomes larger for a mass function $N(m)$ with more abundant massive objects. Thus we can roughly understand the weakly nonlinear correction of power spectrum using information of mass function in the form given in $P_{1h}(0)$.

Note that the present analysis at weakly nonlinear regime $k \leq k_{NL}$ based on equations (32) and (33) does not depend on details of the halo density profile. Therefore in this regime we should not be troubled seriously with potential problems about the reliability of the universal profile for non-Gaussian models. This also means that our analysis is not sensitive to the bias parameter $b(m)$ (eq.[10]). In the region where $u(k,m) = 1$ is a good approximation, we need the bias parameter only in the form of equation (11). But this equation represent a simple requirement that the large-scale fluctuation is analyzed perturbatively $P_{NL}(k) \simeq P_L(k)$. Here we should notice that we have not taken into account the nonlinear biasing effects or the exclusion effects of halo-halo clustering. These effects might be important in weakly nonlinear regime (Scoccimarro et al. 2000), but we neglect them in this

article. At present there is no simple prescription to deal with these two opposite effects. This is a generic problem of the dark-matter-halo approach.

Using results for $n = -2$ model we discuss effects of the linear PDF on the weakly nonlinear evolution of the power spectrum. As shown in figure 1.a the nonlinear correction for the LN2-model is very weak. In this model there are no halos with $m \geq m_*$ (see figure 2) and the integral $\int N(m)m^2dm$ is much smaller than other models. The weakly nonlinear effect is strongest for the LN1-model as expected from its mass function in figure 2. Even at $k \simeq k_{NL}$ magnitude of the nonlinear power spectra can differ by a factor of 10 depending on the initial PDFs.

Next we compare the behavior of nonlinear power spectrum $P_{NL}(k)$ for different spectral indexes n. As n becomes larger, the nonlinear correction becomes smaller (figures 1a-1c). All nonlinear power spectra $P_{NL}(k)$ for $n = -1$ model are very close to the linear spectrum $P_L(k)$, but these for $n = -2$ model depend largely on the adopted PDF. This n-dependence can be also understood by using the integral $P_{1h}(0)$ given in equation (34). We have the following simple relation for the root-mean-square mass fluctuations $\sigma(m)$

$$\frac{\delta_c}{\sigma(m)} = \nu = \left(\frac{m}{m_*}\right)^{(n+3)/6}. \tag{36}$$

As the index n increases, abundance of large mass objects becomes smaller. Then the magnitude of the one-halo term $\simeq P_{1h}(0)$ decreases and we have smaller nonlinear corrections.

4. CDM SPECTRUM

In this section we study nonlinear evolution of the power spectrum for realistic models. We fix the cosmological parameters at $h = 0.7$, $\Omega_0 = 0.3$ and $\lambda_0 = 0.7$ that are compatible with CMB (*e.g.* Lange et al. 2000) and high-redshift SNe data (Riess et al. 1998, Perlmutter et al. 1999). We use the primordially scale invariant ($n = 1$) spectrum with CDM transfer function from Bardeen et al. (1986). The power spectrum is COBE-normalized and we have $\sigma_8 \simeq 0.9$. For these parameters the nonlinear wavenumber k_{NL} defined in equation (28) becomes $k_{NL} = 0.19$Mpc.

Robinson & Baker (2000) studied evolution of the cluster abundance in representative non-Gaussian models, such as, Peebles isocurvature cold-dark-matter (ICDM) model or cosmic string model. This ICDM model corresponds to a χ^2-model with one degree of freedom (see appendix A). Peebles (1999b) show that the power spectrum for this model with parameters $\Omega_0 = 0.2$, $\lambda = 0.8$ and $n_\phi = 2.4$ (see eq. [A14] for definition of n_ϕ) is in good agreement with observed spectrum of CMB and the large-scale structure.

Robinson & Baker (2000) also analyzed PDFs of smoothed linear density fields for these non-Gaussian models and found that the PDFs are well fitted by the log-normal distributions that are nearly scale independent at weakly nonlinear scale. For example, they did not detect scale dependence for the ICDM model and the string+HDM model (their table 1). Thus, motivated by their work, we investigate the log-normal PDFs given in equation (20) and neglect the scale dependence. We characterize the non-Gaussianity of a log-normal PDF by the skewness parameter $S \equiv \langle\delta^2\rangle / \langle\delta^2\rangle^{3/2}$ (see eq.[26]). For models in Robinson & Baker (2000) we can estimate the parameter S from their table 1. We have $S \simeq 2.2$ (somewhat smaller than result $\simeq 2.5$ given in Peebles 1999b) for the ICDM model with $n_\phi = -2.4$ and $S \simeq 0.5$ for the string+HDM model. The parameter S for the ICDM model is larger than the observed constraint $S < 0.52$ (95% CL) given in Feldman et al. (2000). A simple improvement is to increase the number N of scalar fields. This number N corresponds to the degree of freedom in χ^2_N-model. As discussed in appendix A, the parameter S scales are $S \propto N^{-1/2}$ and the required number of freedom N is $N \gtrsim (2.2/0.52)^2 \simeq 20$ (Feldman et al. 2000).

In figure 3.a we show the nonlinear spectrum at the wave number $k = k_{NL}$ as a function of the parameter S. The concentration parameter is fixed at $c(m) = 9(m/m_*)^{-0.13}$ (Bullock et al. 1999). We first calculate the ratio

$$\frac{P_{NL}(k)}{P_L(k)} \equiv \frac{P_{2h}(k) + P_{1h}(k)}{P_L(k)}, \tag{37}$$

in the full dark-matter-halo approach. We also evaluate the simple approximation with putting $u(k, M) = 1$, namely

$$\frac{P_{NL}(k)}{P_L(k)} \simeq 1 + \frac{P_{1h}(0)}{P_L(k)} \tag{38}$$

to check the effects of the bias parameter $b(M)$ and the halo inner density profile $u(k, M)$. As commented before, validity of these two elements for non-Gaussian models have not been clarified numerically so far. The simple approximation (38) shows reasonable agreement with the full result (37) and we can expect that our analysis is not seriously affected by uncertainty of two elements in the framework of the dark-matter-halo approach. Figure 3.a shows that nonlinear spectrum depends strongly on the primordial non-Gaussianity measured by the parameter S. For the Gaussian model ($S = 0$) we have $P_{NL}/P_L \sim 1.3$ but $P_{NL}/P_L \sim 2$ for $S \simeq 1$. For the value $S = 0.52$ (on 95% CL of Feldman et al. 2000) the correction becomes $P_{NL}/P_L \lesssim 1.55$ and about 20% larger than the Gaussian model. We also calculate the ratio P_{NL}/P_L for the Gaussian model using the fitting formula of Peacock & Dodds (1996). The result is ~ 1.2 and close to our result 1.3.

In figure 3.b we show the nonlinear spectrum at the wavenumber $k = 0.66k_{NL}$ where the linear CDM spectrum becomes $P_L(0.66k_{NL}) = 2P_L(k_{NL})$. Apparently the correction

becomes smaller than at $k = k_{NL}$. We can easily understand this fact. At weakly nonlinear scale we have

$$P_{NL}(k) - P_L(k) \simeq P_{1h}(0) \tag{39}$$

and the nonlinear correction behaves as $P_{NL}/P_L \simeq 1 + P_{1h}(0)/P_L(k)$ in the dark-matter-halo approach.

5. SUMMARY

In this article we have studied evolution of the matter power spectrum in non-Gaussian models of structure formation. We have used the dark-matter-halo approach that is an excellent method for analyzing matter clustering from linear to nonlinear scales (Seljak 2000, Ma & Fry 2000b). This approach contains three basic ingredients (i) the mass function $N(m)$ of dark-matter-halos, (ii) the bias factor $b(m)$ of halos relative to the large-scale density fluctuations and (iii) the density profiles $u(k, m)$ of halos. Recent numerical simulations (Robinson & Baker 2000) have suggested that a simple extension of the Press & Schechter formula provides good fits to mass function of clusters also in non-Gaussian models. For the bias factor $b(m)$ and the density profiles $u(k, m)$ it has not checked numerically whether we can simply extend the formulas of Gaussian models to non-Gaussian models. Therefore we take a moderate position to limit our investigation up to weakly nonlinear regimes $k \lesssim k_{NL}$. In these regions our analysis supports that the evolved power spectrum does not depend on details of the bias factor $b(m)$ or the density profile $u(k, m)$.

The nonlinear power spectrum predicted by the dark-matter-halo approach is constituted by two terms. The two-halo term counts two points in different halos and the one-halo term represents contributions of two points within same halos. We have shown that the two-halo term is almost same as the linear power spectrum in weakly nonlinear regimes and nonlinear correction mainly comes from the one-halo term. This term is roughly approximated by the integral of mass function $N(m)$ as $\int N(m)m^2 dm$. Using this integral we can understand various aspects of the weakly nonlinear effect. For example, nonlinear correction is larger than a PDF with more positive tail or smaller spectral index n.

We also study a COBE-normalized CDM spectrum in a flat model ($\Omega_0 = 0.3, \lambda_0 = 0.7$ and $h = 0.7$) with log-normal PDFs. This shape of PDF is motivated by work of Robinson & Baker (2000) who found numerically that PDFs of many representative non-Gaussian models are fitted well by log-normal distributions. We show that the nonlinear spectrum P_{NL} at $k = k_{NL} \simeq 0.2\mathrm{Mpc}^{-1}$ becomes $P_{NL}/P_L = 1.3$ for the Gaussian model but $\simeq 1.55$ for the log-normal model with $S = 0.52$ that is on 95% CL of the observed constraint by Feldman et al. (2000). These results suggest that the ratios P_L/P_{NL} for ΛCDM model at

$k < k_{NL} \simeq 0.2\mathrm{Mpc}^{-1}$ could not largely (say factor of 2) vary within currently allowed region of the primordial non-Gaussianity.

The author would like to thank an anonymous referee for valuable comments to improve this manuscript. My work is supported by Japanese Grant-in-Aid No. 0001416.

A. SCALE DEPENDENCE OF THE SKEWNESS IN χ^2_N-MODELS

The scale dependence of a non-Gaussian PDF becomes highly complicated as it is generally very difficult to deal with infinite degrees of freedom of nonlocal quantities. Here we study the scale dependence of the PDF using the skewness parameter for χ^2_N model.

Let us discuss χ^2_N distribution with N degrees of freedom. The unsmoothed density field $\rho(\boldsymbol{x})$ is written by N independent Gaussian random fields $\phi_i(\boldsymbol{x})$ $(i = 1, \cdots, N)$

$$\rho(\boldsymbol{x}) = \sum_{i=1}^{N} \phi_i(\boldsymbol{x})^2. \tag{A1}$$

We assume that these N fields have same statistical character. Moments of the unsmoothed field $\rho(\boldsymbol{x})$ is given in terms of the variance $\langle\phi_i^2\rangle$ of the basic Gaussian fields ϕ_i (the bracket $\langle\cdot\rangle$ represents ensemble average). We can easily calculate their moments as

$$\begin{aligned} \langle\rho(\boldsymbol{x})\rangle &= N\left\langle\phi_i^2\right\rangle, \quad \left\langle\delta\rho(\boldsymbol{x})^2\right\rangle = 2N\left\langle\phi_i^2\right\rangle^2, \\ \left\langle\delta\rho(\boldsymbol{x})^3\right\rangle &= 8N\left\langle\phi_i^2\right\rangle^3, \quad \left\langle\delta\rho(\boldsymbol{x})^4\right\rangle = (48N + 12N^2)\left\langle\phi_i^2\right\rangle^4. \end{aligned} \tag{A2}$$

where we have defined the overdensity $\delta\rho(\boldsymbol{x})$ by $\delta\rho(\boldsymbol{x}) \equiv \rho(\boldsymbol{x}) - \langle\rho(\boldsymbol{x})\rangle$. Furthermore we can derive the explicit formula for the PDF of ρ as

$$p(\nu)d\nu = \frac{(1 + \nu\sqrt{2N^{-1}})^{N/2-1}}{(2N^{-1})^{(N-1)/2}\Gamma(N/2)} \exp\left(-\frac{N}{2}\left(1 + \sqrt{\frac{2}{N}}\nu\right)\right) d\nu, \tag{A3}$$

where we have defined the normalized overdensity ν by $\nu \equiv \delta\rho/\left\langle\delta\rho^2\right\rangle^{1/2}$ and $\Gamma(\cdot)$ is the Gamma function. As the number N increases, the PDF becomes closer to the Gaussian distribution. This seems reasonable considering the central limit theorem. For smaller degrees of freedom N, the PDFs show strong non-Gaussianity.

The skewness parameter S is a fundamental quantity to characterize the non-Gaussian profile. For χ^2_N-model we have the following expression from equation (A2) for moments

$$S \equiv \frac{\langle\delta\rho(\boldsymbol{x})^3\rangle}{\left\langle\delta\rho(\boldsymbol{x})^2\right\rangle^{3/2}} = \sqrt{\frac{8}{N}}. \tag{A4}$$

Note that using the skewness parameter S, we can specify the χ^2_N-distribution that is completely characterized by the degrees of freedom N.

The simplicities of relations given so far are mainly due to local nature of the density field $\rho(\boldsymbol{x})$. Every statistical characters of the field are reduced to simple Gaussian statistics of the basic fields $\phi_i(\boldsymbol{x})$. When we discuss smoothing effects on the density field $\rho(\boldsymbol{x})$ that is an nonlinear combination of Gaussian fields ϕ_i, the situation becomes highly complicated. First we define the smoothed density field $\rho_R(\boldsymbol{x})$ by

$$\rho_R(\boldsymbol{x}) = \int d\boldsymbol{x}' \rho(\boldsymbol{x}') w(\boldsymbol{x}' - \boldsymbol{x} : R), \tag{A5}$$

where $w(\boldsymbol{x}; R)$ is a filter function with smoothing radius R. In this appendix we mainly use the Gaussian filter

$$w(\boldsymbol{x} : R) = \frac{1}{\sqrt{(2\pi R^2)^3}} \exp\left(-\frac{\boldsymbol{x}^2}{2R^2}\right).$$

We expand the fields $\phi_i(\boldsymbol{x})$ in terms of the Fourier modes $\phi_i(\boldsymbol{k})$

$$\phi_i(\boldsymbol{x}) = \frac{1}{(2\pi)^3} \int d\boldsymbol{k} \phi_i(\boldsymbol{k}) \exp(i\boldsymbol{k}\cdot\boldsymbol{x}). \tag{A6}$$

As the basic fields ϕ_i obey independent random-Gaussian distributions, their statistical nature is completely determined by their power spectrum $P_\phi(k)$ defined by

$$\langle \phi_i(\boldsymbol{k}) \phi_j(\boldsymbol{l}) \rangle = P_\phi(k) \delta_{ij} \delta_D(\boldsymbol{k} + \boldsymbol{l}), \tag{A7}$$

where δ_{ij} is the Kronecker's delta, $\delta_D(\cdot)$ is the Dirac's delta function and we have assumed that fluctuations are isotropic. Similarly the smoothed density field $\rho_R(\boldsymbol{x})$ is written by $\phi_i(\boldsymbol{k})$ as

$$\rho_R(\boldsymbol{x}) = \sum_{i=1}^{N} \frac{1}{(2\pi)^6} \int d\boldsymbol{k} d\boldsymbol{l} \phi_i(\boldsymbol{k}) \phi_i(\boldsymbol{l}) \exp(i(\boldsymbol{k}+\boldsymbol{l})\cdot\boldsymbol{x}) W(|\boldsymbol{k}+\boldsymbol{l}|R), \tag{A8}$$

where $W(kR)$ is the Fourier transformed filter function of $w(\boldsymbol{x} : R)$. For the Gaussian filter we have $W(kR) = \exp(-k^2R^2/2)$. With expression (A8) we can write down the second- and third-order moments for the smoothed density field in terms of the power spectrum $P_\phi(k)$. After some algebra we arrive at

$$\langle \delta\rho_R^2 \rangle = \frac{2N}{(2\pi)^6} \int d\boldsymbol{k} d\boldsymbol{l} P_\phi(k) P_\phi(l) W(|\boldsymbol{k}+\boldsymbol{l}|R)^2, \tag{A9}$$

$$\langle \delta\rho_R^3 \rangle = \frac{8N}{(2\pi)^9} \int d\boldsymbol{k} d\boldsymbol{l} d\boldsymbol{m} P_\phi(k) P_\phi(l) P_\phi(m) W(|\boldsymbol{k}+\boldsymbol{l}|R) W(|\boldsymbol{l}+\boldsymbol{m}|R) W(|\boldsymbol{m}+\boldsymbol{k}|R). \tag{A10}$$

Using these equations we evaluate the skewness parameter S_R for the smoothed density field. We can easily confirm that the unsmoothed value $S = \sqrt{8/N}$ is recovered by setting

$R = 0$ in these equations. The smoothing effect changes the skewness parameter S_R from the unsmoothed value $S = \sqrt{8/N}$. To discuss quantitative effects of smoothing we define a parameter f_R defined by

$$S_R \equiv \frac{\langle \delta\rho_R(\boldsymbol{x})^3 \rangle}{\langle \delta\rho_R(\boldsymbol{x})^2 \rangle^{3/2}} = \sqrt{\frac{8}{f_R N}}. \tag{A11}$$

Note that the parameter f_R does not depend on the degrees of freedom N. The effective degrees of freedom N' determined form the smoothed skewness parameter S_R becomes f_R times original value.

Next let us evaluate the smoothed skewness S_R numerically and the scaling parameter f_R for a sequence of matter fluctuations. We adopt the following from for the power spectrum of the Gaussian fields ϕ_i

$$P_\phi(k) = Ak^{n_\phi} \exp(-k^2 r^2). \tag{A12}$$

As the normalization factor A is irrelevant for our linear analysis we simply put $A = 1$. Due to the Gaussian cut-off $\exp(-k^2r^2)$, small scale power at wave-number $k \gtrsim r^{-1}$ is strongly suppressed and the fields $\phi_i(\boldsymbol{x})$ and $\rho(\boldsymbol{x})$ are very smoothed at spatial scale smaller than r. This means that the smoothed density field $\rho_R(\boldsymbol{x})$ is close to the unsmoothed field $\rho(\boldsymbol{x})$ for smoothing radius R with $R \lesssim r$. Therefore radius r represents the spatial scale where the PDF of the smoothed field ρ_R would become close to the original χ^2_N distribution and the scaling factor would be $f_R \sim 1$.

Using equation (A9) for variance of the smoothed density field, we obtain the following result for the Gaussian filter

$$\left\langle \delta\rho_R^2 \right\rangle = \frac{NR^{-6-2n_\phi}}{4\pi^4} \int_0^\infty ds \int_0^\infty dt (st)^{n_\phi+1} \exp\left[-\left(1 + \frac{r^2}{R^2}\right)(s^2+t^2) \right] \sinh(2st). \tag{A13}$$

At large smoothing radius R we have $\langle (\delta\rho)^2 \rangle \propto R^{-6-2n_\phi}$ and the matter power spectrum at small wave-number would behave as (Peebles 1999b, White 1999, Scoccimarro 2000)

$$P_\rho(k) \propto k^{2n_\phi+3} = k^{n_\rho}, \tag{A14}$$

where we have defined the spectral index n_ρ of density field by $n_\rho \equiv 2n_\phi + 3$.

The expression (A10) for the third-order moment is a nine-dimensional integral. But using symmetry with respect to variables $\boldsymbol{k}, \boldsymbol{l}$ and $\boldsymbol{m}$, we can simplify the expression. After some algebra we arrive at

$$\begin{aligned} \left\langle \delta\rho_R^3 \right\rangle &= \frac{NR^{-9-3n_\phi}}{4\pi^6} \int_0^\infty ds \int_0^\infty dt \int_0^\infty du \int_0^\pi da \sin a \int_0^\pi db \sin b (stu)^{2+n_\phi} I_0(tu \sin a \sin b) \\ &\quad \times \exp\left[-\left(1 + \frac{r^2}{R^2}\right)(s^2+t^2+u^2) - (st\cos a + tu\cos a\cos b + us\cos b) \right], \end{aligned} \tag{A15}$$

where $I_0(x)$ is the 0-th modified Bessel function. From equations (A13) and (A15), it is apparent that the factor f_R is written in the form

$$f_R = f(R/r). \tag{A16}$$

In the large scale limit $R \to \infty$, the small scale Gaussian cut-off in the power spectrum $P_\phi(k)$ (eq.[A12]) would have no effects on the second- and third-order moments as expected from equations (A13) and (A15). In this limit we can put $r = 0$ and our results should coincide with results for pure power-law models $P_\phi(k) \propto k^{n_\phi}$ (Peebles 1999b, Scoccimarro 2000). Simple analytic expressions for the matter power spectrum P_ρ and bispectrum B_ρ for $n_\phi = -2$ model are given by Scoccimarro (2000) as follows

$$P_\rho(k) = \frac{2\pi^3 N}{k}, \quad B_\rho(\boldsymbol{k}, \boldsymbol{l}, \boldsymbol{m}) = \frac{8\pi^3 N}{klm}. \tag{A17}$$

With the latter expression we can numerically study the third-order moment $\langle(\delta\rho_R)^3\rangle$ at $R \to \infty$. In this case we need only two-dimensional numerical integration that is much simpler than the five-dimensional integration (A15). We find the numerical result [3]

$$f(\infty) = 2.6 \quad (n_\phi = -2). \tag{A18}$$

This asymptotic value can be used to check our five-dimensional numerical integration required to evaluate the smoothed skewness at an intermediate scale.

In figure 4 we show scale dependence of the factor $f(R/r)$ for power spectrum (A12) with various spectrum indices, $n_\phi = -1$, $n_\phi = -1.5$, $n_\phi = -2$ and $n_\phi = -2.4$. These indices correspond to $n_\rho = 1$, $n_\rho = 0$, $n_\rho = -1$, and $n_\rho = -1.8$, respectively. The last choice $n_\phi = -2.4$ is same as Peebles (1999b). As expected, we have $f(R/r) \simeq 1$ for $R \lesssim r$ reflecting the original profile of the unsmoothed PDF. For a larger smoothing radius $R \gtrsim 20r$ the parameter $f(R/r)$ relaxes to an asymptotic value $f(\infty)$ that does not depend on the small scale cut-off as explained earlier. The asymptotic value for $n_\phi = -2$ model is close to the value given in equation (A18) and show the validity of our numerical integration. Peebles (1999b) calculated the skewness parameter smoothed by the top-hat filter for a model with one degree of freedom $N = 1$ and spectral index at $n_\phi = -2.4$, using Monte Carlo integration. His result is $S_R = 2.46$ and corresponds to $f_R \simeq 1.32$. This value is close to our asymptotic value $f(\infty) \simeq 1.37$ obtained for the Gaussian filter.

As shown in figure 4, the factor $f(R/r)$ largely depends on the spectral indices n_ϕ. We have $f(\infty) \simeq 200$ for $n_\phi = -1$ ($n_\rho = 1$) model. This large value indicates that the

[3]For the top-hat filter we have similar result $f(\infty) = 2.6$.

PDF would become close to the Gaussian profile. The factor keeps $f(R/r) \lesssim 3$ for $n_\phi = -2$ ($n_\rho = -1$) model. White (1999) investigated this model using N-body simulations and found that the PDF is skewed for Gaussian smoothing spanning a factor 5 in scale. This behavior is consistent with our result. For $n_\phi = -2.4$ model, the factor $f(R/r)$ changes only $\sim 40\%$ in the range $0 \leq R < \infty$. These dependence on the spectral indices n_ϕ seems reasonable considering that as n_ϕ increases, number of statistically independent region would also increases for a given smoothing volume and the PDF would become a more Gaussian like profile.

REFERENCES

Albrecht, A. 2000, preprint (astro-ph/0009129)

Avelino, P. P. & Viana, P. T. P. 2000, MNRAS, 314, 354

Balbi, A. et al. 2000, preprint (astro-ph/0005124)

Bond, J. R., Cole, S. Efstathiou, G. & Kaiser, N. 1991, ApJ, 379, 440

Bouchet, F. R., Peter, P., Riazuelo, A. & Sakellariadou, M. 2000, preprint (astro-ph/0005022)

Bullock, J. S. et al. 1999, preprint (astro-ph/9908159)

Chiu, W. A., Ostriker, J. P. & Strauss, M. A. 1998, ApJ, 482, 479

Chodorowski, M. J. & Bouchet, F. R. 1996, MNRAS, 279, 557

Contaldi, C. R., Ferreira, P. G., Magueijo, J. & Górski, K. M. 2000, ApJ, 534, 25

Cooray, A., Hu, W. & Miralda-Escude, J. 2000, ApJ, 535, L9

Cooray, A., & Hu, W. 2000, preprint (astro-ph/0004151)

Durrer, R., Juszkiewicz, R., Kunz, M., & Uzan, J. 2000, Phys.Rev.D, 58, 021301

Feldman, H. A., Frieman, J. A., Fry, J. N. & Scoccimarro, R. 2000, preprint (astro-ph/0010205)

Ferreira, P. G., Górski, K. M. & Magueijo, J. 1998, ApJ, 503, L1

Fry, J. N. & Scherrer, R. J. 1994, ApJ, 429, 36

Fukushige, T. & Makino, J. 1997, ApJ, 477, L9

Hamilton, A. J. S. Matthews, A., Kumar, P. & Liu, E. 1991, ApJ, 374, L1

Jain, B., Mo, H. & White, S. D. M. 1995, MNRAS, 276, L25

Jenkins et al. 2000, preprint (astro-ph/0005260)

Jing, Y. P. & Suto, Y. 2000, ApJ, 529, L69

Kaiser, N. 1984, ApJ, 284, L9

Komatsu, E. & Kitayama, T. 1999, ApJ, 526, L1

Koyama, K. Soda, J. & Taruya, A. 1999, MNRAS, 310, 1111

Kravtsov,A. V. & Klypin, A. 1999, ApJ, 520, 437

Lacey, C. & Cole, S. 1993, MNRAS, 262, 627

Lange, A. et al. 2000, preprint (astro-ph/0005004)

Linde, A. & Mukhanov, V. 1997, Phys.Rev.D, 56, 535

Lucchin, F. & Mataresse, S. 1989, ApJ, 330, 535

Ma, C-P. & Fry, J. N. 2000a, ApJ, 531, L87

Ma, C-P. & Fry, J. N. 2000b, preprint (astro-ph/0003343)

Ma, C-P. & Fry, J. N. 2000c, preprint (astro-ph/0005233)

Makino, N., Sasaki, M. & Suto, Y. 1992, Phys.Rev.D, 46, 585

Matarrese, S., Verde, L. & Jimenez, R. 2000 preprint (astro-ph/0001366)

McClelland, J. & Silk, J. 1977, ApJ, 217, 331

Mo, H. & White, S. D. M. 1996, MNRAS, 282, 347

Mo, H. Jing, Y. P. & White, S. D. M. 1997, MNRAS, 284, 189

Moore, B. et al. 1998, ApJ, 499, L5

Moore, B. et al. 1999, MNRAS, 310, 1147

Navarro, J. F., Frenk, C. S. & White, S. D. M. 1996, ApJ, 462, 563

Navarro, J. F., Frenk, C. S. & White, S. D. M. 1997, ApJ, 490, 493

Peacock, J. A. & Dodds, S. J. 1996, MNRAS, 280, L19

Peacock, J. A. & Smith, R. E. 2000, preprint (astro-ph/0005010)

Peebles, P. J. E. 1974, A&A, 32, 197

Peebles, P. J. E. 1997, ApJ, 483, L1

Peebles, P. J. E. 1999a, ApJ, 510, 523

Peebles, P. J. E. 1999b, ApJ, 510, 531

Perlmutter, S. et al. 1999, ApJ, 517, 565

Press, W. H. & Schechter, P. 1974, ApJ, 187, 425

Riess, A. G. et al. 1998, AJ, 116, 1009

Robinson, J. Gawiser, E & Silk, J. 1998, preprint (astro-ph/9805181)

Robinson, J. Gawiser, E & Silk, J. 2000, ApJ, 532, 1

Robinson, & J. Baker, J. E. 2000, MNRAS, 311, 781

Saunders, W. et al. 2000, MNRAS, 317, 55

Scherrer, R. J. & Bertschinger, E. 1991, ApJ, 381, 349

Scoccimarro, R. 2000, preprint (astro-ph/0002037)

Scoccimarro, R. Sheth, R. K., Hui, L. & Jain, B. 2000, preprint (astro-ph/0006319)

Seljak, U. 2000, preprint (astro-ph/0001493)

Sheth, R. & Lemson, G. 1999, MNRAS, 304, 767

Sheth, R. & Tormen, B. 1999, MNRAS, 308, 119

Sheth, R. et al. 2000, preprint (astro-ph/0009167)

Srednicki, M. 1993, ApJ, 416, L1

Vachaspati, T. 1986, Phys.Rev.Lett., 57, 1655

Verde, L. Wang, L. Heavens, A. F. & Kamionkowski, M. 2000, MNRAS, 313, 141

Vilenkin, A. 1985, Phys.Rep., 121, 263

White, M. 1999, MNRAS, 310, 511

White, M. 2000, preprint (astro-ph/0005085)

Willick, J. A. 2000, ApJ, 530, 80

This preprint was prepared with the AAS LaTeX macros v5.0.

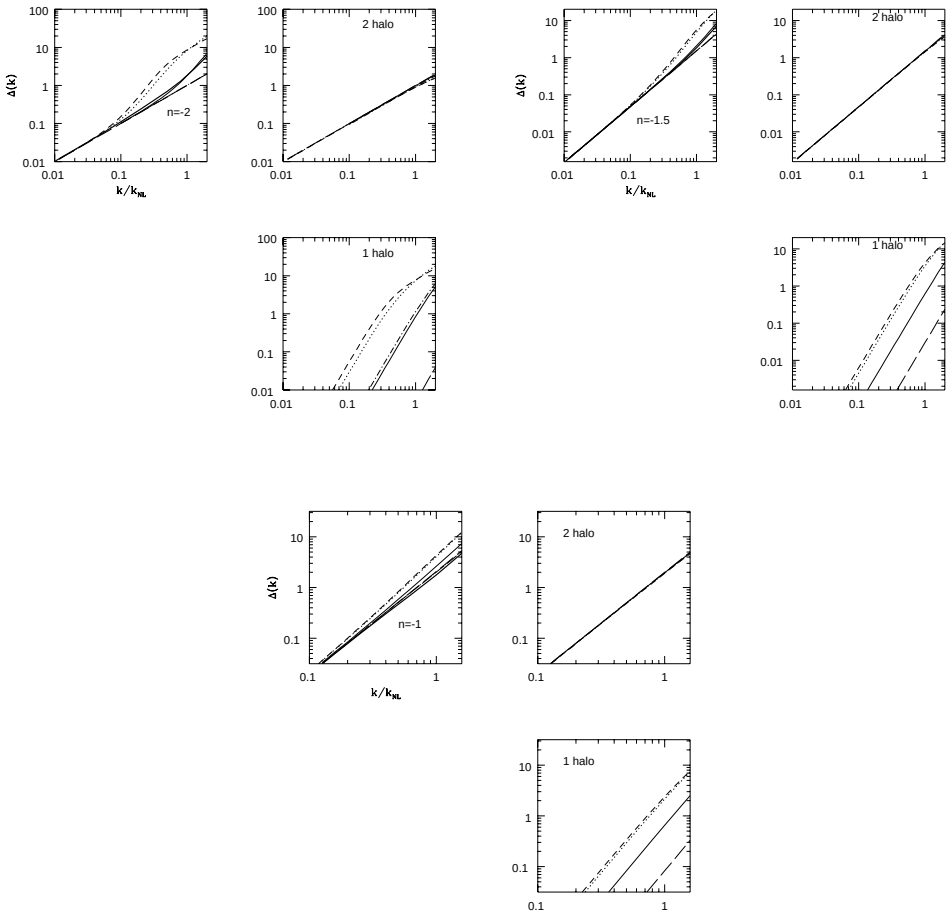

Fig. 1.— Nonlinear power spectrum $\Delta(k) \equiv P_{NL}(k)k^3/(2\pi^2)$ for $n = -2$ model (fig.1a), $n = -1.5$ model (fig.1b), $n = -1$ model (fig.1c). In the right panels we plot the two-halo and one-halo terms separately. The total values (summations of two terms) are presented in the left panels. Dash-dotted lines represent the linear spectra. Thin solid lines correspond to the G-model, dotted-lines to the C-model, short-dashed lines to the LN1-model and long-dashed lines to the LN2-model. The thick-solid lines are obtained from the fitting formula of Peacock & Dodds (1996) given for Gaussian fluctuations. In the left panels the long-dashed lines (LN-2 model) and the dash-dotted lines (linear spectra) are nearly overlapped.

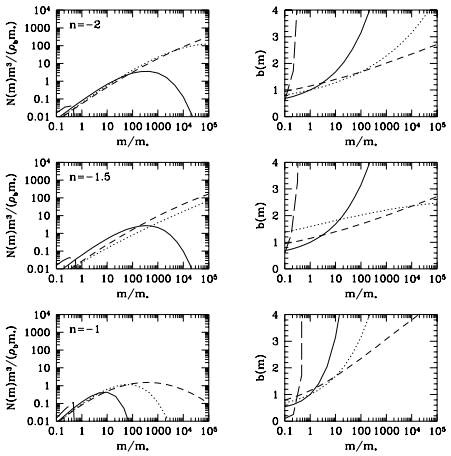

Fig. 2.— The mass functions and the bias parameters for various PDFs. Correspondence of lines and models is same as figure 1. There are no halos with $m \geq m_*$ in the LN2-model. We plot the mass function $N(m)$ in the form $N(m)m^3$, as the integral $\int N(m)m^2dm$ is important for our analysis.

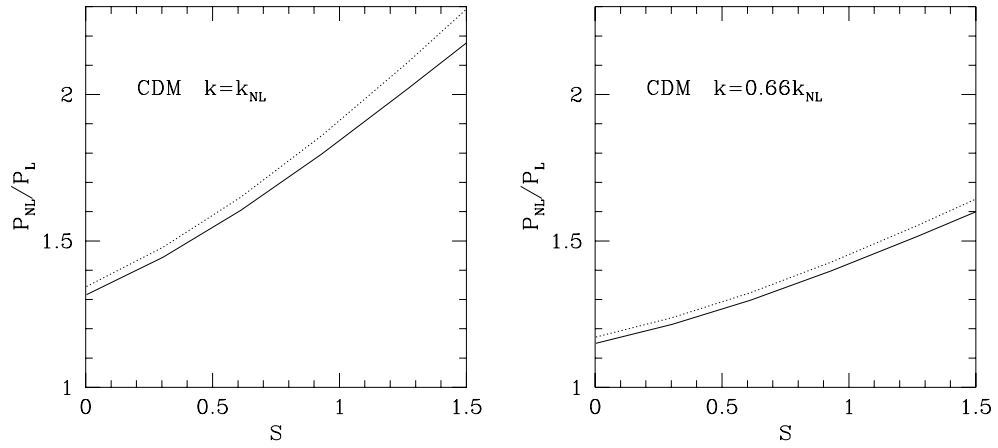

Fig. 3.— Nonlinear spectrum for non-Gaussian initial fluctuations with CDM spectra. We characterize the non-Gaussianity by the skewness parameter S. The ratio P_{NL}/P_L is given at $k = k_{NL}$ (fig 3.a) and $k = 0.66k_{NL}$ (fig 3.b). The solid lines represent the results from full dark-matter-halo approach and the dotted lines are obtained by the simple approximation described in the main text.

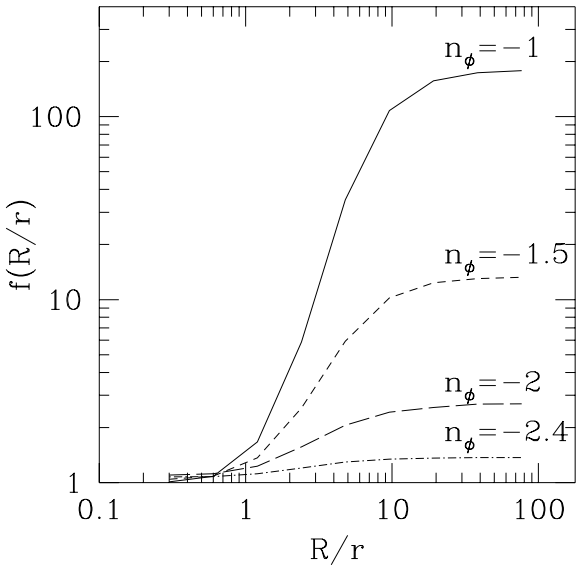

Fig. 4.— The scaling factor $f(R/r)$ (see eq.[A11]) as a function of Gaussian smoothing radius R. We have $f(R/r) \sim 1$ for $R/r > 1$ and $f(R/r) \sim const$ for $R/r > 20$.